
FAILURE ANALYSIS OF A GARAGE DOOR SPRING

AME 60646: Failure of Materials

Matt Landrigan

1 December, 2006

Abstract

A 2005 U.S. census reported 124.5 million housing units in the United States. Countless millions include garages with garage doors. A mechanism necessary for proper function of the garage door is the spring; either one torsion spring or two extension springs are used. In May of 2006, an extension spring hook failed while the garage door was being lifted at a house on Rockne Drive in South Bend. The failure was a result of fatigue and corrosion with multiple initiation sites in the tensile region of the hook. The cracks came together to create a single crack front that propagated to the point of catastrophic failure. As a fairly cheap part with limited criticality, emphasis is not placed on fatigue life and therefore failure could be expected.

Description of the Failure

In May of 2006, an extension garage door spring fractured completely through rendering the door unusable until repair. A garage door operates with either two extension springs on either side of the bracket supports or one torsion spring across the top of the door frame. The motor for this particular setup drives a screw gear that pushes the door down when it closes putting tension into the spring (Fig. 1a). The springs are connected to a wire cable which runs over two pulleys redirecting the spring force along the curve of the door track. The springs aid the motor in lifting the door by placing an upward force on the door. The last coil of the spring is bent to form a hook (Fig. 1b).

Nothing unusual occurred on the day of the failure. Unfortunately, no information was available regarding manufacturer, installation date, type of material, or fatigue life although it is safe to say that the fracture is due to fatigue failure since the springs were installed when the house was purchased in May 2005. Both springs are identical looking so it is likely they are the original springs. The door was even lifted with only one spring a couple of times before it was realized that one was broken. The motor was likely installed at a later time than the springs due to modern electrical wiring – an indication that perhaps in the past the loading pattern was not as rigorous as in modern day life. Replacement springs (Overhead Door Company – parent company to Genie Company, motor manufacturer) at the local hardware store are rated for 10,000 cycles. Assuming the springs were installed when the house was built and a conservative usage estimate of



Fig. 1. (a) Installed garage door extension spring in relaxed position. (b) View of operational spring with circle designating area of fracture.

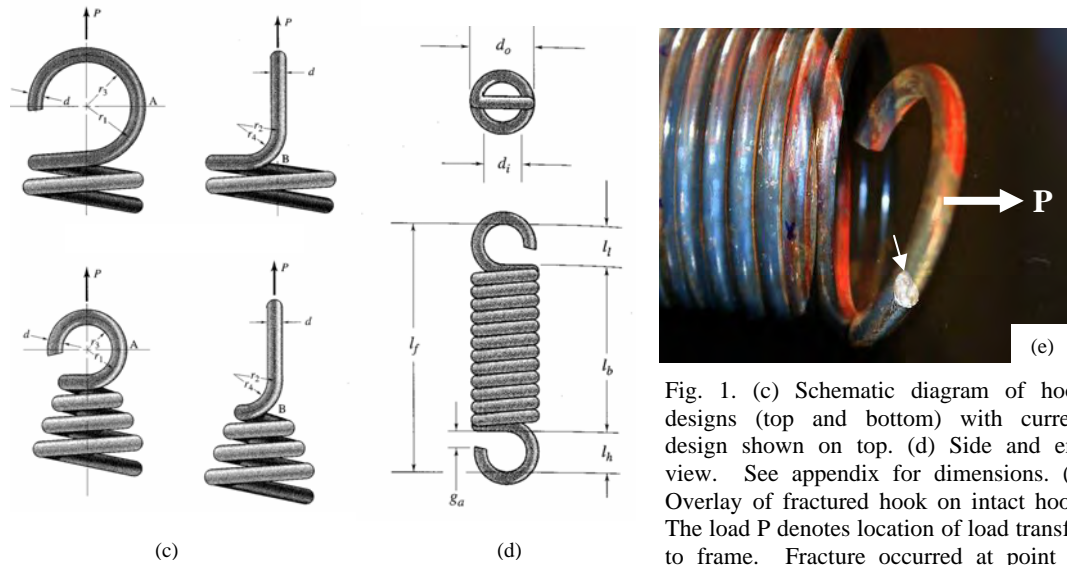


Fig. 1. (c) Schematic diagram of hook designs (top and bottom) with current design shown on top. (d) Side and end view. See appendix for dimensions. (e) Overlay of fractured hook on intact hook. The load P denotes location of load transfer to frame. Fracture occurred at point of maximum stress on inside of hook (arrow).

one complete cycle per day yields a fatigue life of 27 years – exactly half of the age of the house. Although it is impossible to know the exact loading history, a proposition could be made that since the pace of life has increased, the door may not actually have been used every day; it may have even been used solely for storage especially if a garage door motor wasn't attached in which case the springs would have seen even less usage. Coincidentally, if the door were used on average every other day, a 10,000 cycle rated spring would last exactly 54 years – in this case from 1952 to 2006.

Helical extension springs are nothing more than a metal wire coiled around in loops. In the manufacturing process, an initial tension is incorporated to pull the coils tight against each other. The initial tension allows the spring to be consistent in length and taught so it doesn't wobble when unloaded. The initial tension is wound into the spring by bending the wire away from its normal coiling direction causing a small twist in the wire. The small twist causes the coils to spring back against the next coil¹.

Most often helical extension springs fail at the hook and the design of the end hook impacts the stress concentration. This particular spring hook was manufactured by simply bending the last coil outward by 45 degrees. In idealized spring design, the end hook is bent outward forming a right angle with the plane of the previous coil. In the loading condition for this spring design the 45° angle causes a torque to act on the hook as well as the axial load (Fig. 1e). This was an important aspect used to determine the initiation region which will be discussed momentarily. Purely axial loading normally causes failure at the tensile edge furthest from the neutral axis. If a torque is added, the maximum stress shifts around the hook slightly due to the addition of the shear stress.

Crack Initiation/Propagation Mechanisms

Both fracture surfaces were recovered and aided in the failure analysis. The surface proved to be quite complex with multiple modes of fracture indicative of the highly three dimensional surface (Fig. 2a-b). Areas of fatigue failure and brittle fracture exist. Observation under SEM revealed multiple crack initiation sites. The surface attached to the spring (Fig. 2a) was largely corroded with rust and therefore less visual information was available. The end attached to the hook proved invaluable because optical microscopy revealed rust bands on the inside of the hook – the area of maximum stress (Fig. 2b - circle 1). The rust rings follow two distinct centers (Fig. 2d, pointers) with radial marks leading outward from the centers. The rust rings are separated by a ratchet mark - a ledge between two initiation sites (Fig. 3c-d). Ratchet marks are indicative of initiation sites although it is normal to find beach marks around the marks (Fig. 2e) but there can be radial marks instead (Fig. 2f). As the crack planes propagate, the two planes come together forming a single fracture plane (Fig. 4c).

Inclusions, second phase particles, voids, machining marks or other surface flaws, and geometric anomalies are typical fatigue crack initiation points. Due to surface rust on the outside of the hook, a specific initiation type could not be determined. Because the initiation sites are at the surface, the cracks likely would have initiated because of a surface flaw such as a tooling mark or surface pit which could easily have been caused by corrosion.

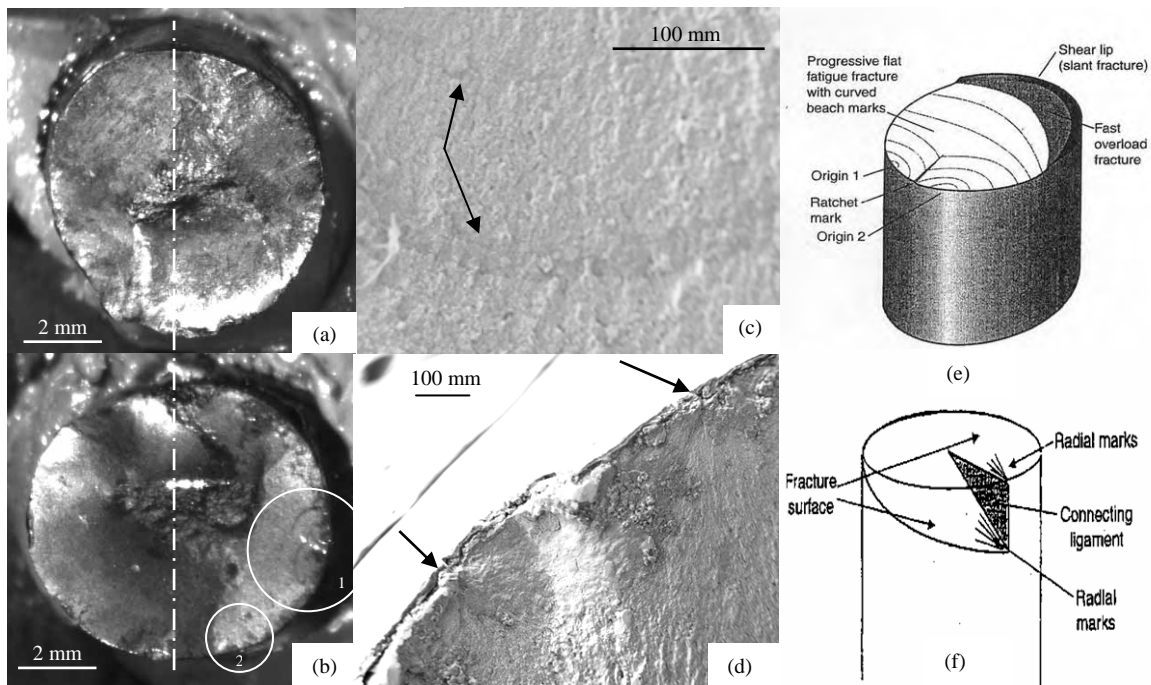


Fig. 2. (a) Optical image of surface attached to spring and (b) surface of hook end. The right hand side was in tension. The white dashed line indicates neutral axis and the circle shows the region of initiation. (c) SEM image of rust bands. (d) SEM image of initiation points (pointers) surrounding ratchet mark (white region). Pictorial representations of ratchet marks and beach marks (e)⁷ and radial marks (f)⁸.

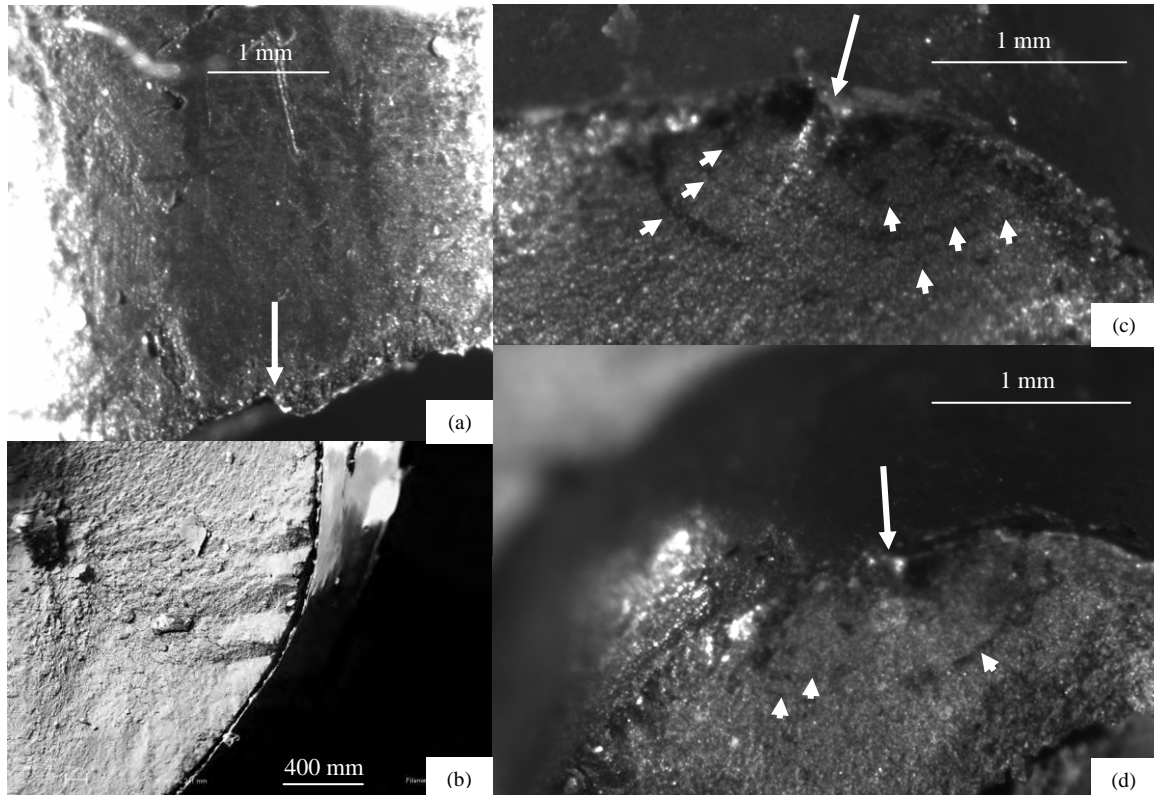


Fig. 3. Fatigue initiation sites. (a) Ratchet mark (arrow) around which rust rings formed. (b) SEM image of multiple ratchet marks from area 2 in Fig. 4b. (c) Fracture surface connected to hook end and (d) surface on spring end. Small markers indicate rust rings and large arrow points to ratchet mark.

The other area of interest is circle number 2 (Fig. 2b) where multiple ratchet marks can be seen under optical microscopy and closer under SEM (Fig. 3b). The location for the ratchet lines is understandable because the combined torque and tensile loading of the hook moves the maximum stress region around the outside of the hook closer to the neutral axis.

There are three different loading modes by which cracks can form and propagate as shown in Fig. 4a. Mode I is the tensile opening mode, Mode II is the in-plane shearing mode, and Mode III is the out-of-plane shearing mode². With the initiation sites in the tensile region of the hook (Fig. 4c) and the fracture surface perpendicular to the wire direction (Fig. 5), Mode I failure is responsible for the crack initiation.

There are two distinct regions of crack propagation. The presence of rust rings indicated that the crack propagated slowly and allowed time for corrosion to materialize. The fracture surface plane is perpendicular to the wire direction (Fig. 5) showing Mode I crack propagation initially. About one third of the way across the fracture surface (Fig. 4c), the crack switches to Mode II or possibly Mode III failure. The fracture plane switches directions on an angle called the shear lip as shown schematically in Fig. 4b and for this particular surface in Fig. 5. At the same time the crack propagated very quickly

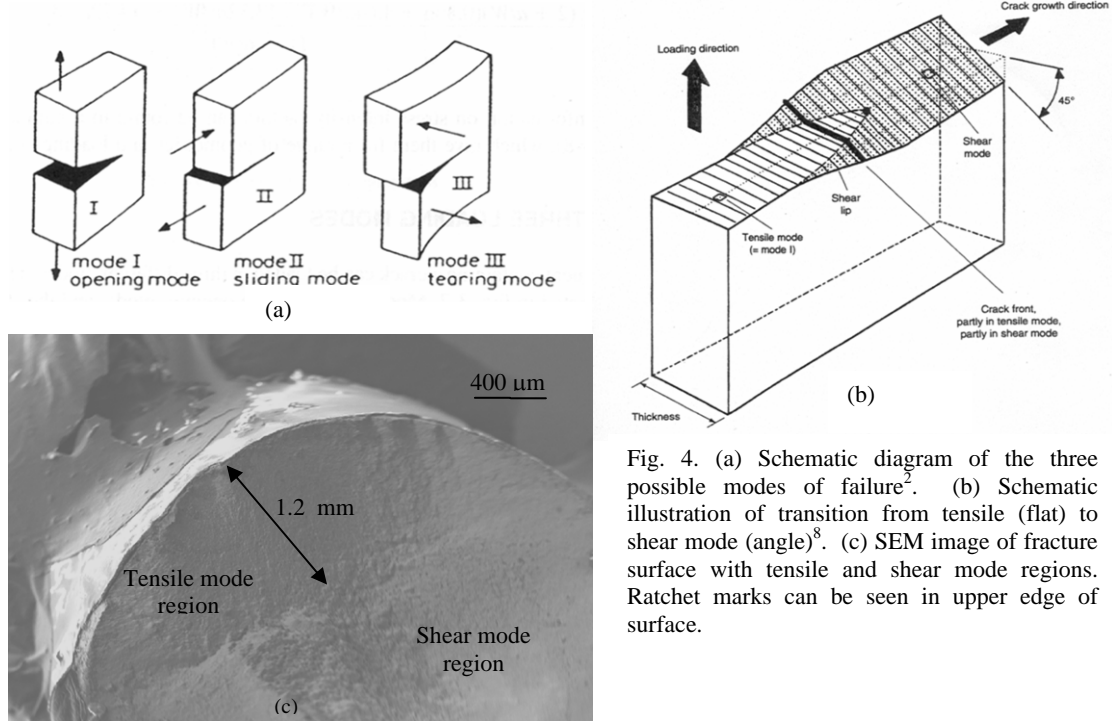


Fig. 4. (a) Schematic diagram of the three possible modes of failure². (b) Schematic illustration of transition from tensile (flat) to shear mode (angle)⁸. (c) SEM image of fracture surface with tensile and shear mode regions. Ratchet marks can be seen in upper edge of surface.

because the fracture surface is rough in this region compared to the area around the rust rings indicating catastrophic failure occurred when the crack switched failure modes.

Engineering Calculations

Electrical Dispersive Spectrometry (EDS) was performed on a polished and etched sample. Accurate element compositions were not obtained because the EDS reported a carbon content of about seven percent and iron only ninety percent. Most steels have carbon contents less than one percent. Music wire, oil-tempered, and hard-drawn spring wire are the three most common types of spring wire. Hard drawn spring steels are the lowest quality of the three types and are typically used for cost savings, and where long fatigue life and uniformity are not as important¹ – exactly the type which would be a good candidate for this application.

To confirm that the spring was well within operating conditions, a Vickers microhardness test was performed per ASTM E92-03¹¹. A small wire sample was

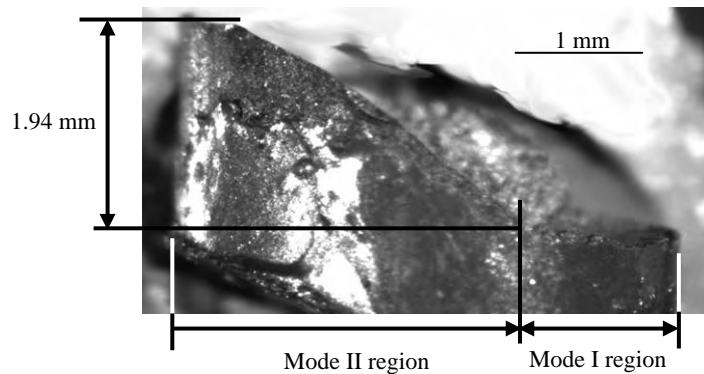


Fig. 5. Side view of fracture surface where Mode I and Mode II regions are visible.

taken a few millimeters below the fracture surface on the spring side of the failure. The sample was embedded and polished to a one micrometer surface finish. The microhardness testing was performed with a one kilogram load for ten seconds. Hardness measurements taken from the center of the wire to the outside edge on the tensile side (Fig. 6) showed uniform strength throughout with an average Vickers hardness number of 488. Converting to Brinell hardness (HB) yields a hardness number of 459.¹⁰ Brinell hardness can be used to estimate the tensile strength (TS) of a material⁴:

$$TS(\text{MPa}) = 3.45 \times \text{HB} \quad (1)$$

This analysis proved very useful because of the lack of background information on the spring material. Using this correlation between the hardness and tensile strength resulted in a tensile strength of 1583 MPa. The standard extension spring stress recommendation for hard drawn steel wire (Fig. 7) of diameter 4.3 mm in light service is 780 MPa, half of the tensile strength. In addition, the range for class 1 hard drawn wire⁵ is 1360-1560 MPa and therefore, from a theoretical point of view, the spring was well within the design parameters for this application with similar properties to the hard-drawn steel alloy 4340.

Two approximations were developed to calculate the maximum stress in the hook^{3,1}.

$$\sigma_A = \left(\frac{Mc}{I} \right) \left(\frac{r_1}{r_3} \right) + \frac{P}{A} = \left(\frac{32P_A r_1}{\pi d^3} \right) \left(\frac{r_1}{r_3} \right) + \frac{4P_A}{\pi d^2} = 879 \text{ MPa} \quad (2)$$

$$\sigma_A = \frac{5PD^2}{ID \cdot d^3} = 840 \text{ MPa} \quad (3)$$

These stress calculations represent the upper limit because the load used is the total load of the door. However, the gear and motor do pull up on the door some so the actual load

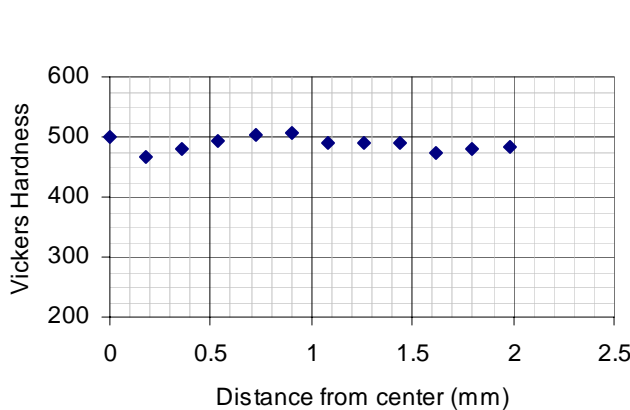


Fig. 6. Results of Vickers Hardness test. Measurements were taken from the center and extending in the radial direction toward the region of maximum tension.

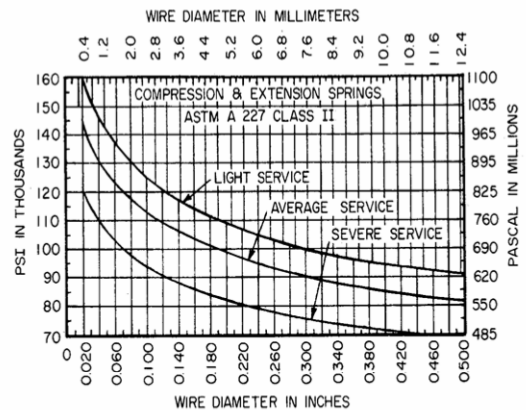


Fig. 7. Recommended design stresses for hard-drawn steel wire – based on ASTM A 227 for compression and extension springs¹.

transferring through the extension springs is less than the weight of the door. If the motor pulls up as little as 10% of the door weight, that reduces the stress to 790 MPa, essentially the same as recommended in Fig. 7. The motor likely pulls up even more because after the spring failed, the door was lifted a couple of times with only one operational spring and the motor.

The allowable tensile yield stress can be estimated as 60% of the ultimate tensile strength^{1,3} resulting in $\sigma_{ty} = 950$ MPa. Under perfect conditions this would ensure the integrity of the spring and fatigue failure would not be an issue. Obviously the hook did fail because of several flaws accompanied by corrosion.

An estimate of the fracture toughness can be made by looking at the fast fracture region of the failed surface. If an elliptical flaw geometry propagating from the edge is assumed⁹, the fracture toughness can be calculated by Eq. 4:

$$K_I = 1.12\sigma\sqrt{\pi a} \quad (4)$$

where σ is the far-field stress and a is the crack length. The fracture toughness, K_{IC} , for Steel Alloy 4340 is $50 \text{ MPa}\sqrt{m}$. Under the hook stress calculated in Eq. 3 and a K_{IC} of $50 \text{ MPa}\sqrt{m}$, the critical crack length to induce catastrophic failure is 1.03 mm (Fig. 8). It should be noted that the Mode I region of failure (Fig. 4c) has a depth of 1.2 mm. Although this isn't exactly the same length, they are on the same order indicating that the fracture toughness estimate is a good approximation.

One last examination into the fracture toughness is based on the plastic zone size or the shear lip width. Once the mode of failure turns to the shear state, the crack propagates quickly and catastrophic failure is imminent. Therefore, the height of the shear lip can be used to calculate the fracture toughness⁷. Assuming a plane stress state, a first approximation relating the stress, fracture toughness, and plastic zone size is given as:

$$r_y = \frac{1}{2\pi} \left(\frac{K_I}{\sigma_y} \right)^2 \quad (5)$$

This equation is erroneous because as the crack tip displacement goes to zero, the stress at the crack tip goes to infinity. To accommodate this, a second approximation was

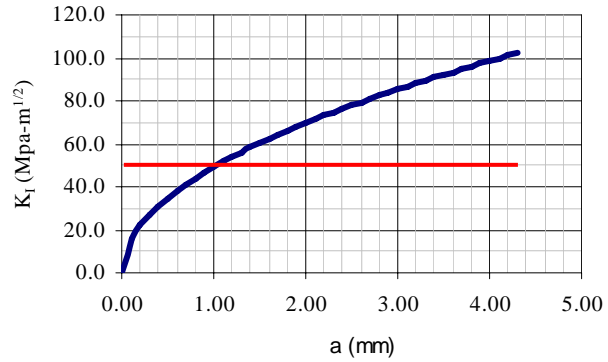


Fig. 8. The effect of the flaw size on the fracture toughness, K_I using the stress from Eq. 3. K_{IC} approximation is in grey.

developed under the assumption that the maximum stress at the crack tip can not be greater than the yield stress resulting in a larger plastic zone region:

$$r_y = \frac{1}{\pi} \left(\frac{K_I}{\sigma_y} \right)^2 \quad (6)$$

Using the height of the shear region shown in Fig. 5 and Eq. 6 above, along with the hook stress calculated earlier gives a fracture toughness of $64 \text{ MPa}\sqrt{m}$. While this would indicate that the spring steel has a stronger fracture toughness than assumed earlier, it is close and therefore a reasonable approximation for the toughness of the spring steel.

The spring failed in fatigue where several initiation sites were responsible for opening cracks. The cracks coalesced together forming one large crack surface which propagated slowly in Mode I failure. Once the crack length increased enough that the fracture toughness of the steel was eclipsed fast fracture occurred on the the shear plane.

Redesign or Failure Prevention Strategy

In reality, this part is very cheap to manufacture and currently retails for about \$15 at the local hardware store. Because it is likely that this spring has lasted at least 27 years, but more likely 54 years, it really would not be cost effective to improve the fatigue life. That being said, the easiest way to improve the fatigue life would be to put tighter manufacturing requirements to avoid tooling marks or other possible surface marks. Secondly, altering the wire material itself improves the fatigue life. Another way to increase the fatigue life is to reduce the stress in the spring hook. Reducing the moment arm (see Eq. 2) such as in Fig. 1c will drastically reduce the stress on the hook. These three aspects will increase the fidelity of the spring, but in this particular application it is not practical to spend the extra manufacturing time and money to improve the fatigue life.

References

1. Carlson, H. Spring Designer's Handbook, Marcel Dekker, INC., New York, 1978.
2. McEvily, A. Metal Failures: Mechanisms, Analysis, Prevention, John Wiley & Sons, Inc., New York, 2002.
3. Hamrock, B., Jacobson, B., and Schmid, S. Fundamentals of Machine Elements, McGraw Hill, New York, 1999.
4. Callister, W.D. Materials Science and Engineering: An Introduction, John Wiley & Sons, Inc., New York, 2000.
5. ASTM Standard A 227/A 227/M - 99. Standard Specification for Steel Wire, Cold-Drawn for Mechanical Springs. 1999.
6. Maker, J.H. Failure of Springs. Metals Handbook, Vol. 11, ASM International, ASM Handbook, 550-562, 1986.
7. Becker, W.T. Fracture Appearance and Mechanisms of Deformation and Fracture. Metals Handbook, Vol. 11, ASM International, 559-583, 2000.
8. Lund, R.A. Fatigue Fracture Appearances. Metals Handbook, Vol. 11, ASM International, 627-637, 2000.
9. Anderson, T.L. Fracture Mechanics: Fundamentals and Applications, 2nd Ed. CRC Press LLC, New York, 1995.
10. ASTM Standard E 140-05. Standard Hardness Conversion Tables for Metals Relationship Among Brinell Hardness, Vickers Hardness, Rockwell Hardness, Superficial Hardness, Knoop Hardness, and Scleroscope Hardness. 2005.
11. ASTM Standard E92-03. Standard Test Method for Vickers Hardness of Metallic Materials. 2003.

Appendix

Table 1. Hook dimensions corresponding to Fig. 1c-d and stress equations.

| Dimension | Value |
|-----------|---------|
| r_1 | 17.5 mm |
| r_3 | 15.4 mm |
| d | 4.3 mm |
| d_i | 30.8 mm |
| d_o | 39.4 mm |
| P | 334 N |